# Spatio-Temporal Changes in River Dynamics and Land Cover Along the Seti River Floodplain, Kaski District, Nepal (1989–2017)

Bikash Adhikari[1], Aastha Singh Bhandari[1], Ram Chandra Tiwari[2], and Aanchal Tiwari[2*]

[1]Department of Environmental Science and Engineering, Kathmandu University, Nepal
[2]Department of Civil Engineering, Institute of Engineering, Pulchowk Campus, Tribhuvan University, Lalitpur, Nepal

(*Corresponding E-mail: 079mstre001.aanchal@pcampus.edu.np)

**Abstract: This study examines decadal changes (1989–2017) in river dynamics and land cover along the Seti floodplain, Kaski District, using GIS and Remote Sensing. The Seti River's sinuosity decreased over time, with bank shifts ranging from 6.7 m to 42.7 m, while land cover changes included increases in water bodies (7.60→8.34 km²), built-up areas (32.44→80.98 km²), agriculture and grassland (251.21→320.15 km²), and snow/glacier (458.05→477.55 km²), and decreases in barren land (353.80→332.07 km²) and shrub/forest (984.75→889.05 km²).**

**Keywords:** ***Land use and land cover change (LULC), Seti floodplain, Remote sensing and GIS, Bankline shift, Spatio-temporal changes.***

## Introduction

Land use and land cover (LULC) changes, driven by natural and human activities, alter surface properties, river systems, and water availability (Zewdu et al., 2016). Urbanization further converts agricultural lands to built-up areas, impacting social and ecological stability (Deng et al., 2009). Remote sensing and GIS enable analysis and visualization of land cover and river dynamics (Barnsley, 1999). Indices like NDVI, NDWI, and NDSI are used to classify and monitor LULC changes. Various indices are used for the proper delineation of land cover in GIS.

NDVI (λ) is an indicator of live green vegetation, calculated from red (λ = 550–700 nm) and near-infrared reflectance. Healthy plants absorb red light and strongly reflect NIR, allowing NDVI to assess vegetation presence and vigor.

$$NDVI = \frac{R_{NIR} - R_{Red}}{R_{NIR} + R_{Red}} = \frac{Band_4 - Band_3}{Band_4 + Band_3} \quad (1)$$

Where RNIR is the reflectance of NIR radiation and RRED is the reflectance of visible red radiation (Govaerts and Verhulst, 2010). NDSI identifies snow cover by comparing green and shortwave infrared (SWIR) reflectance. Snow reflects strongly in visible/NIR but absorbs in SWIR, allowing accurate mapping of snow extent.

$$NDSI = \frac{R_{Green} - R_{SWIR}}{R_{Green} + R_{SWIR}} = \frac{Band_2 - Band_5}{Band_2 + Band_5} \quad (2)$$

Where $R_{Green}$ is the reflectance of visible green radiation and RSWIR is the reflectance of shortwave infrared radiation.

NDWI identifies and highlights open water by comparing green and near-infrared (NIR) reflectance, reducing interference from soil and vegetation, and can also indicate water turbidity (McFeeters, 1996).

$$NDWI = \frac{R_{Green} - R_{NIR}}{R_{Green} + R_{NIR}} = \frac{Band_2 - Band_4}{Band_2 + Band_4} \quad (3)$$

Where $R_{Green}$ is the reflectance of visible green radiation and $R_{NIR}$is the reflectance of near infrared radiation.

## Material and Method

Kaski District, in Nepal's Gandaki region (Province 4), spans 2,017 km² between 28.2622° N and 84.0167° E, with elevations from 450 m to 8,901 m. Its administrative center and headquarters is Pokhara. River dynamics were assessed by measuring sinuosity and bank line shifts to evaluate channel migration, curvature, and lateral movement along the river. The detailed procedure is illustrated in the flow chart (Figure 1). Figure 2 shows the sections of the Seti River.

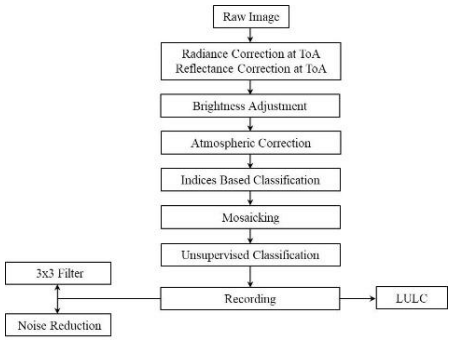


*Figure 1, Methodology Flow chart*

The extent to which a river channel departs from a straight line is known as river sinuosity (Ebisemiju, 1994). It is calculated as follows.

$$\text{Sinuosity}(S) = L/l \quad (3)$$

Where L=Total length of a reach and l= length of straight line between the two points.

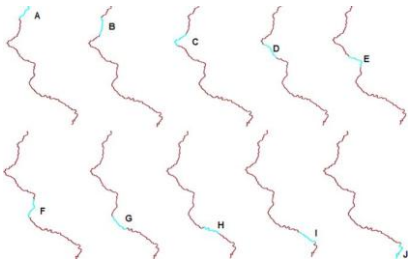


*Figure 2, Sections of River.*

## Results and Discussion

After the application of the radiometric corrections, clear and good quality images were obtained for the analysis (Figure 3). Figure 4 shows the section wise sinuosity of Seti from 1989 to 2017. Figure 5 shows the section wise bank shift of Seti from 1989 to 2017.

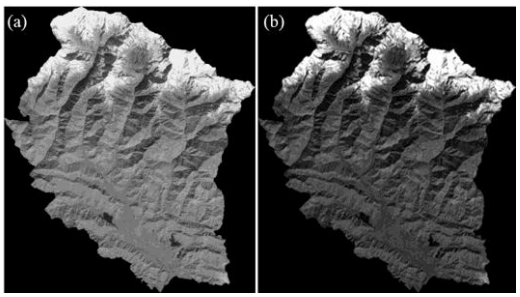


*Figure 3, Image correction: (a) Before and (b) After.*

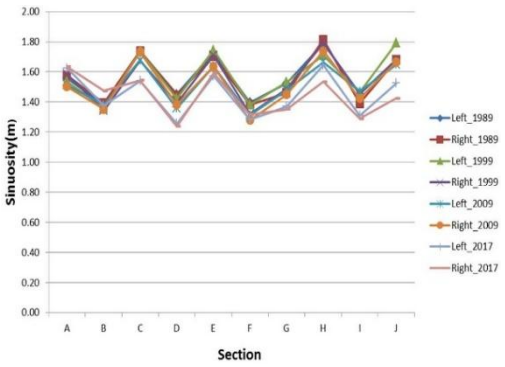


*Figure 4, Section wise sinuosity of Seti from 1989 to 2017.*

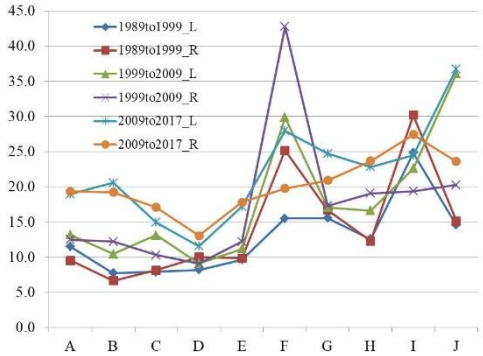


*Figure 5, Section wise bank shift of Seti from 1989 to 2017.*

From 1989 to 2017, the Seti River's sinuosity decreased with maximum bank shifts up to 42.7 m, while LULC changes show shrub/forest (984.75→889.05 km²) and barren land (353.80→332.07 km²) declining, and built-up (32.44→80.98 km²), agriculture (251.21→320.15 km²), water (7.60→8.34 km²), and snow/glacier (458.05→477.55 km²) increasing, reflecting urbanization and geomorphic changes.

## Conclusion

GIS analysis (1989–2017) in Kaski District shows shrub and forest decline (47.17→42.17%) and built-up growth (1.55→3.84%), with agricultural areas gradually expanding. The meandering Seti River exhibits significant bank shifts, posing risks to settlements and highlighting the need for timely LULC and river dynamics assessment for sustainable management.

## References

Barnsley, M. (1999). Digital remotely-sensed data and their characteristics. Geographical Information Systems, 1, 451–466.

Deng, J. S., Wang, K., Hong, Y., and Qi, J. G. (2009). Spatio-temporal dynamics and evolution of land use change and landscape pattern in response to rapid urbanization. Landscape and Urban Planning, 92(3), 187–198. https://doi.org/10.1016/j.landurbplan.2009.05.001

Ebisemiju, F. S. (1994). The sinuosity of alluvial river channels in the seasonally wet tropical environment: Case study of river Elemi, southwestern Nigeria. Catena, 21 (1), 13–25. https://doi.org/10.1016/0341-8162(94)90028-0

Govaerts, B., and Verhulst, N. (2010). The normalized difference vegetation index (NDVI) Greenseeker™ handheld sensor: Toward the integrated evaluation of crop management. Part A—Concepts and case studies. CIMMYT.

McFeeters, S. K. (1996). The use of the Normalized Difference Water Index (NDWI) in the delineation of open water features. International Journal of Remote Sensing, 17 (7), 1425–1432. https://doi.org/10.1080/01431169608948714

Zewdu, S., Suryabhagavan, K. V., and Balakrishnan, M. (2016). Land-use/land-cover dynamics in Sego Irrigation Farm, southern Ethiopia: A comparison of temporal soil salinization using geospatial tools. Journal of the Saudi Society of Agricultural Sciences, 15 (1), 91–97. https://doi.org/10.1016/j.jssas.2014.03.003